PERGAMON

Engineering Fracture Mechanics 67 (2000) 155–168

Engineering Fracture Mechanics

www.elsevier.com/locate/engfracmech

A complete Gurson model approach for ductile fracture ☆

Z.L. Zhang *, C. Thaulow, J. Ødegård

SINTEF Materials Technology, Rich. Birkelands vei 1C, N-7465 Trondheim, Norway

Received in revised form 31 March 2000

Abstract

Recently, a complete Gurson model has been introduced by the authors. The complete Gurson model is a combination of the modified Gurson model which deals with microvoid nucleation and growth, and a physical microvoid coalescence criterion based on the plastic limit load model by Thomason. By comparing finite element cell modeling analyses, the complete Gurson model is accurate for both non-hardening and hardening materials. One attractive feature of the complete Gurson model is that material ductile failure is exclusively linked to the microvoid nucleation parameter, and the nucleation parameter in many cases can be determined without metallurgical examinations. Furthermore, the so-called critical void volume fraction f_c, has been eliminated from material constants. In this paper, two simple microvoid nucleation models for modeling ductile fracture are discussed, and a method which applies multi-tension specimens including both smooth and notched cylindrical specimens for determining the microvoid nucleation parameter is introduced. Once the microvoid nucleation parameter has been determined from the tension specimens, the characteristic length parameter which describes the stress/strain gradient effect can be fitted from fracture mechanics tests. Material ductile crack resistance behavior is then a function of the microvoid nucleation parameter, the length parameter and the specimen geometry. For modified boundary layer models, it has been found that the crack resistance curves can be normalized by the T stress, and the T stress can be possibly taken as the geometry controlling parameter for ductile crack growth.

Keywords: Complete Gurson model; Ductile fracture; Nucleation parameter; Length parameter; Microvoid coalescence criterion; T stress

1. Introduction

It is a known fact that the macroscopic parameter for ductile fracture, such as ductility and crack resistance curve cannot be directly transferred from one geometry to another. One of the important tasks is thus to separate transferable parameters for ductile fracture from the parameters which describe geometry effect. For most engineering alloys, ductile fracture often comes after the nucleation, growth and coalescence of microvoids. It is therefore more reasonable to link ductile fracture to the parameters which describe the

☆ Paper presented at the 1998 HSE/TWI Structural Integrity Seminar, 21 October 1998, Abington, Cambridge, UK. The original title for the paper was "Some recent advances in the Gurson model approach".

* Corresponding author. Tel.: +47-73-59-25-30; fax: +47-73-59-29-31.

E-mail address: zhiliang.zhang@matek.sintef.no (Z.L. Zhang).

0013-7944/00/$ - see front matter
PII: S0013-7944(00)00055-2

micro-ductile fracture mechanisms than to the macroscopic pseudo fracture parameters. The Gurson model [1] is one of the widely known micromechanical models for ductile fracture. With modifications by many authors, particularly by Tvergaard and Needleman [2–4], however, the Gurson model can only simulate the microvoid nucleation and growth, and has no intrinsic ability to predict void coalescence. The reason for the failure to predict void coalescence is that only a homogenous deformation mode was considered in deriving the Gurson model. One remedy for this insufficiency is to use an empirical void coalescence criterion – void coalescence occurs when a critical void volume fraction f_c, has reached. The f_c was selected beforehand or numerically fitted from tension tests [4,5]. However, there was no experimental and numerical evidence to support the supposition that f_c is independent of stress state [6]. Furthermore, it has been clearly shown in finite element cell model analyses [7,8] that f_c strongly depends on initial void volume fraction.

Recently, the plastic limit load model proposed by Thomason for void coalescence [9–11] has received attention. Thomason pointed out that the localized deformation state of void coalescence is very different to the homogenous deformation state during void nucleation and growth, and the homogenous and localized deformation modes should be considered together in modeling ductile fracture. By neglecting the void shape effect and assuming voids are always spherical, a complete Gurson model is obtained by integrating the modified Gurson model and the void coalescence criterion by Thomason. By a modification to Thomason's coefficient, the complete Gurson model has been shown to be very accurate for both low and high stress triaxiality, for both non-hardening and hardening materials.

In the complete Gurson model void coalescence is not determined by any critical value. The so-called f_c is not a material constant, but the material response at void coalescence. Therefore, ductile fracture is exclusively linked to the void nucleation parameter. In this paper, cylindrical smooth and notched tension specimens where the strain gradient is relatively low have been proposed to fit the void nucleation parameter. For a cluster void nucleation model where the voids are nucleated from inclusions and particles at the beginning of plastic deformation, and a continuous void nucleation model where the amount of voids nucleated is proportional to the equivalent plastic strain increment, there is only one void nucleation parameter and the parameter can be uniquely determined. Once the void nucleation parameter has been determined, the remaining characteristic length parameter which describes the strain gradient effect can be fitted from fracture mechanics tests. The void nucleation parameter and the resulting length parameter are the transferable parameters for ductile fracture.

In the following, the complete Gurson model and the relation between the void nucleation parameter and ductile failure are described first. Some new results of a systematic verification study on the complete Gurson model are reported. A method which applies the so-called ductility diagram for determining the nucleation parameter is introduced in Section 3. The method of determining the parameters for modeling ductile crack resistance is discussed in Section 4. Conclusions as well as limitations of the approach are presented at the end.

2. The complete Gurson model

The Gurson model was derived from an approximate limit-analysis of a hollow sphere made of ideal-plastic Mises material [1]. Homogenous boundary strain rate loading was applied to the hollow sphere. The yield function of the Gurson model has the following form:

$$\phi(q,\overline{\sigma},f,\sigma_m)=\frac{q^2}{\overline{\sigma}^2}+2q_1 f\cosh\left(\frac{3q_2\sigma_m}{2\overline{\sigma}}\right)-1-(q_1 f)^2=0, \tag{1}$$

where f is the void volume fraction, which is the average measure of a void-matrix aggregate, σ_m is the mean normal stress, q is the conventional von Mises equivalent stress, $\overline{\sigma}$ is the flow stress of the matrix material, q_1, q_2 are constants introduced by Tvergaard [2,3].

For existing voids, the Gurson model can describe the softening effect caused by the voids on material behavior, and at the same time can predict the void growth rate during plastic deformation. Because the matrix material is incompressible, the growth rate of the existing voids is

$$\mathrm{d}f_{\mathrm{growth}} = (1-f)\mathrm{d}\varepsilon^{\mathrm{p}} : \mathbf{I}, \tag{2}$$

where ε^{p} is the plastic strain tensor and $\mathbf{I}$ is the second-order unit tensor.

Before any growth, voids should be nucleated first – the Gurson model should be "told" when the voids start to nucleate and the amount of voids to be nucleated. Different materials may have different nucleation laws. Void nucleation can be stress controlled or strain controlled. In the literature, strain controlled nucleation has been preferred, because it is easier to handle in the finite element implementation. The strain controlled nucleation can be written:

$$\mathrm{d}f_{\mathrm{nucleation}} = f_{\varepsilon}(\bar{\varepsilon}^{\mathrm{p}})\mathrm{d}\bar{\varepsilon}^{\mathrm{p}}, \tag{3}$$

where f_{ε} is the void nucleation intensity, and $\bar{\varepsilon}^{\mathrm{p}}$ is the equivalent plastic strain. For many engineering materials which contain large inclusions, for example, manganese sulfide or aluminum oxide, voids can be nucleated from the easy-to-break inclusions during the early stage of plastic deformation. For these materials, a cluster model may be used to simulate the void nucleation, Fig. 1(a). In the cluster void nucleation model, voids are assumed to be nucleated at the beginning of plastic deformation and the corresponding parameter is called the initial void volume fraction, f_0 (for the problem with very high hydrostatic stress, the cluster nucleation model is different to the case with pre-existing voids). For materials where voids are nucleated from carbides or intermetallic phases, a continuous void nucleation model may be applied, Fig. 1(b). In this model, the amount of voids nucleated is assumed to be proportional to the increment of equivalent plastic strain, $A_0 = \mathrm{d}f/\mathrm{d}\bar{\varepsilon}^{\mathrm{p}}$. The continuous model may sound crude and has not received much attention in the literature. However, both early and recent experimental work has shown that the model is realistic for many materials, for both steels and aluminum alloys [12,13].

It must be noted that the total volume fraction of the voids nucleated, $\int_0^{\varepsilon_{\mathrm{f}}} f_{\varepsilon}\,\mathrm{d}\bar{\varepsilon}^{\mathrm{p}}$, where ε_{f} is the fracture strain, should be smaller than the total volume fraction of available inclusions/particles for nucleation, f_{v}. In reality, not all the inclusions/particles will nucleate voids, but only some of them. This implies that the f_{v} from metallurgical examination cannot be directly used as the void nucleation parameter in the Gurson model. The nucleation parameter in the Gurson model should be fitted according to materials macroscopic fracture behavior.

A more sophisticated nucleation model which involves more than one parameter has been suggested by Chu and Needleman [14]. The nucleation models shown in Fig. 1 are more attractive because they have only one parameter. As will be discussed later in the paper, this parameter can be uniquely determined.

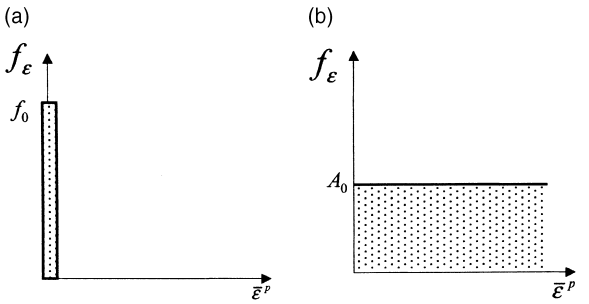

Fig. 1. Void nucleation models for engineering materials: (a) the cluster nucleation model characterized by the initial void volume fraction f_0 and (b) the continuous nucleation model characterized by A_0.

After a certain amount of void growth of the nucleated voids, a sudden drop of material load carrying capacity will follow void coalescence. For most engineering alloys, coalescence occurs at a relatively low void volume fraction (<0.1). The Gurson model, however, cannot predict the sudden material capacity loss at any realistic void volume fraction. One empirical treatment of void coalescence in the Gurson model assumes the void coalescence to occur when a critical void volume fraction, f_c has been reached. The void coalescence will be finished (material load carrying capacity becomes zero) when the void volume fraction reaches another value – the volume fraction at final failure, f_F. For a particular material point when the f_c is known, Tvergaard and Needleman [4] suggested that the effect of coalescence (sudden drop of material load carrying capacity) can be numerically simulated by an artificially accelerated void growth:

$$f^* = \begin{cases} f & \text{for } f \leqslant f_c, \\ f_c + \frac{f_u^* - f_c}{f_F - f_c}(f - f_c) & \text{for } f > f_c, \end{cases} \tag{4}$$

where $f_u^* = 1/q_1$. Koplik and Needleman [7] has shown that Eq. (4) works very well for low stress triaxiality cases, slightly worse for high stress triaxiality cases.

In general, the global numerical response is not very dependent on the value of f_F [15], especially for the cases where stress triaxiality is low. Recently, the authors have carried out plain strain cell model analyses to investigate the value of f_F. Some results are shown in Fig. 2. In Fig. 2, points marked with a circle indicate the starting point of void coalescence, and the point when the normalized current neck dimension becomes zero, indicates the separation of material and the end of coalescence. For the cases analyzed, it can be seen that the minimum value of f_F is about 0.15. From Fig. 2, we may obtain the following approximate relation for f_F:

$$f_F = 0.15 + 2f_0. \tag{5}$$

For the continuous void nucleation model, no approximate relation for f_F exists. However, a fixed value for f_F, for example, $f_F = 0.15$, can be used.

For materials that follow the cluster nucleation law, the unknown parameters are f_0 and f_c. If f_c can be assumed to be a material constant and can be determined beforehand, the only unknown parameter is f_0.

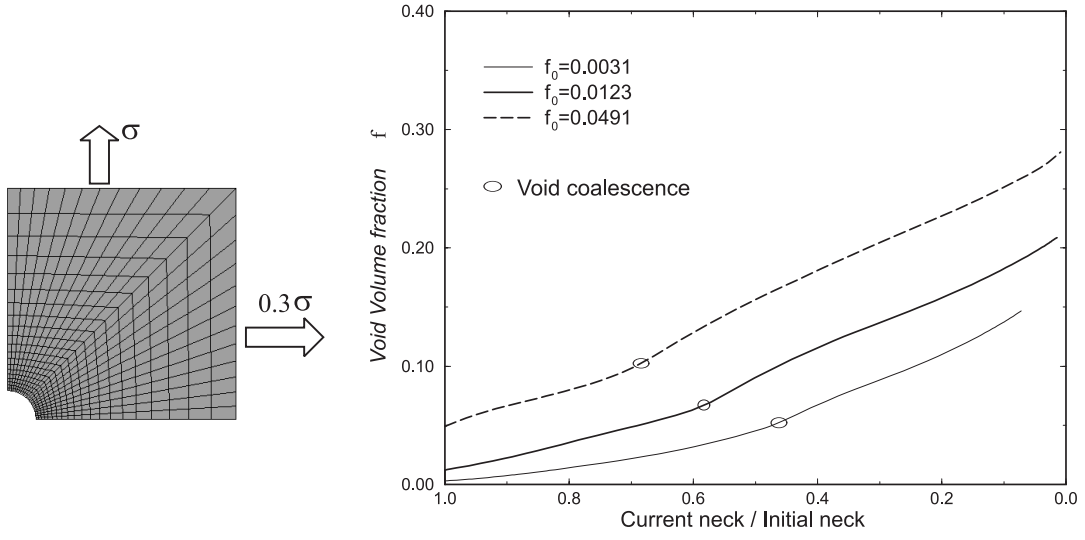

Fig. 2. Void volume fraction versus current neck dimension from cell model FEM analyses. When the normalized current neck dimension becomes zero, it means material separation. The hardening exponent for the matrix material is $n = 0.1$.

However, it is very questionable to assume f_c is a material constant, and numerical study has clearly demonstrated that f_c is a strong function of f_0. The authors have shown that if f_c is fitted from tension tests as suggested in the literature, an infinite number of pairs of (f_0, f_c) can give identical predictions. This non-uniqueness problem is attributed to the failure of the Gurson model to automatically predict void coalescence.

The reason for the failure is that only homogenous deformation modes have been considered in deriving the Gurson model. As argued by Thomason [9], the localized deformation mode of void coalescence should be treated differently. He suggested that the localized deformation mode can be described by the so-called plastic limit load model. The stage of void coalescence depends on the competition between the two deformation modes. In the early stage of deformation, the voids are small and it is easier to follow the homogenous deformation mode (the stress required for going to homogenous deformation is less than the stress required for going to a localized deformation mode). With the advance of plastic deformation and the increase of void volume fraction, the stress required for localized deformation decreases. When the stress for localized deformation is equal to the stress for homogenous deformation, a bifurcation point is reached and the void coalescence will occur. The plastic limit load criterion by Thomason for coalescence for a general 3D problem at a specific material point can be written as follows [8,9]:

$$\frac{\sigma_1}{\overline{\sigma}} < \left(\alpha\left(\frac{1}{r}-1\right)^2 + \frac{\beta}{\sqrt{r}}\right)(1-\pi r^2), \tag{6a}$$

void coalescence will not occur. However, when

$$\frac{\sigma_1}{\overline{\sigma}} = \left(\alpha\left(\frac{1}{r}-1\right)^2 + \frac{\beta}{\sqrt{r}}\right)(1-\pi r^2), \tag{6b}$$

void coalescence starts to occur, and the current void volume fraction will be taken as the f_c. In Eq. (6), σ_1 is the current maximum principal stress, r is the void space ratio, $r = \sqrt[3]{(3f/4\pi)e^{\varepsilon_1+\varepsilon_2+\varepsilon_3}}/\left(\sqrt{e^{\varepsilon_2+\varepsilon_3}}/2\right)$ and ε_1 is the maximum principal strain, ε_2, and ε_3 are the two other principal strains, $\alpha = 0.1$ and $\beta = 1.2$ are constants fitted by Thomason [9]. For plane strain problem, Eq. (6) can still be used, but with $\varepsilon_3 = 0$.

By integrating Eqs. (1)–(6), a complete Gurson model is obtained, in the sense that the model can simulate the complete process of ductile fracture, including void nucleation, growth and coalescence. In the complete Gurson model, void nucleation and growth are described by Eqs. (2) and (3), void coalescence is controlled by Eq. (6), and post-coalescence behavior (effect of coalescence on load carrying capacity) is simulated by Eq. (4). In the complete Gurson model, the f_c is still used. However, here f_c is not a material constant, but a field quantity. In fact, Eq. (4) is not essential to the complete Gurson model. It is used for the matter of convenience. Node release or element removal techniques can be used instead of Eq. (4) [17].

The complete Gurson model has been verified [8] for non-hardening material against the finite element results by Koplik and Needleman [7]. It was found that the complete Gurson model was very accurate, in particular, for small initial void volume fraction cases. Recently, a systematic verification of the complete Gurson model for materials with different hardening has been carried out. Both 2D axisymmetric finite element model and 3D model with solid elements have been carried out. Five hardening cases, $n = 0.0$, 0.05, 0.1, 0.15 and 0.2 were considered. Both large initial void volume fraction and small initial void volume fraction were assessed. Fig. 3 compares the finite element cell model analysis results with the prediction by the complete Gurson model for hardening $n = 0.1$ and 0.2. Detailed results will be reported elsewhere.

Fig. 3 shows that for a given stress triaxiality, the coalescence strain will increase with the increase of strain hardening. The Thomason criterion based on non-hardening material ($\alpha = 0.1$) is accurate for low stress triaxiality cases, but will underestimate the coalescence strain for hardening materials at high stress triaxiality. A similar finding has been reported in a recent work by Pardoen and Hutchinson [16] where the effect of initial void shape on void coalescence has also been studied. Pardoen and Hutchinson have shown

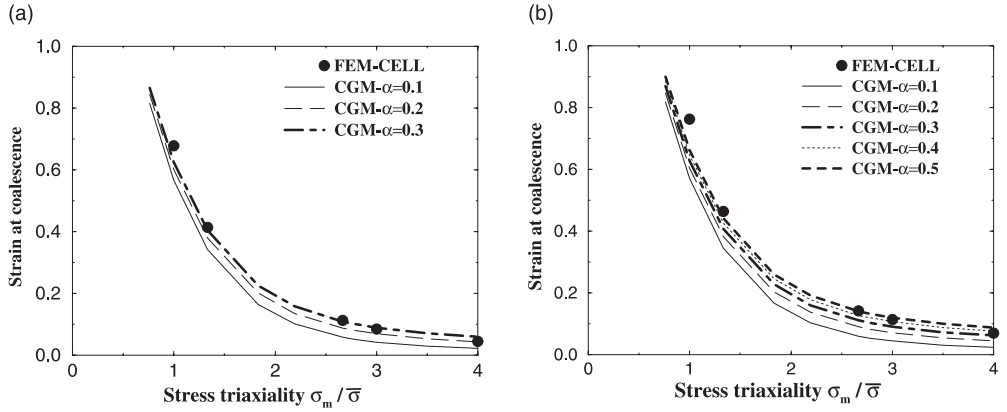

Fig. 3. Comparison of the prediction by the complete Gurson model and the results of axisymmetric cell model FEM analysis: (a) $n = 0.1$ and (b) $n = 0.2$. In the complete Gurson model, $q_1 = 1.25$ and $q_2 = 1.0$, and initial void volume fraction $f_0 = 0.0031$.

that better prediction of void coalescence can be obtained by taking the two coefficients in Eq. (6) as a function of hardening exponent: $\alpha(n)$, $\beta(n)$. They found $\alpha(n) = 0.1 + 0.217 + 4.83n^2$ and $\beta = 1.24$ fits best in average sense to all the cases they studied, where the void shape, hardening and initial void volume fraction were varied. Fig. 3 also shows that the prediction by the complete Gurson model can be improved by increasing the α for hardening material. In the complete Gurson model, the voids are assumed to be always spherical. By considering only the hardening effect, we found the following linear function with $\beta = 1.2$ fits very well to all the cases we analyzed:

$$\alpha(n) = 0.12 + 1.68n. \tag{7}$$

3. A method for determining void nucleation parameter

When the Gurson model is applied to the ductile fracture problem, one needs to determine both the void nucleation parameter and crack tip mesh size which describe the stress–strain gradient. One approach used in the literature is to determine the nucleation parameter from a fracture mechanics test, by selecting a crack tip mesh size. It is obvious that the determined nucleation will be different if another mesh size is applied. In this paper, we pursue such an idea that for the same material, Gurson model should work both at low stress triaxiality case (tensile specimens) and high stress triaxiality case (cracked specimens). The void nucleation parameter can therefore be determined from tensile specimens where the mesh size has no significant effect. In the following a new method for determining void nucleation parameter from tensile specimens is discussed.

3.1. Single specimen approach

The advantage of the complete Gurson model is that ductile failure is exclusively controlled by the nucleation parameter and geometry, and the so-called critical void volume fraction has been eliminated from material constants. Instead, the f_c has become a field quantity. For a tension specimen with a cluster nucleation model, the ductility can be expressed as

$$\varepsilon_f = \varepsilon_f(f_0, G, n), \tag{8}$$

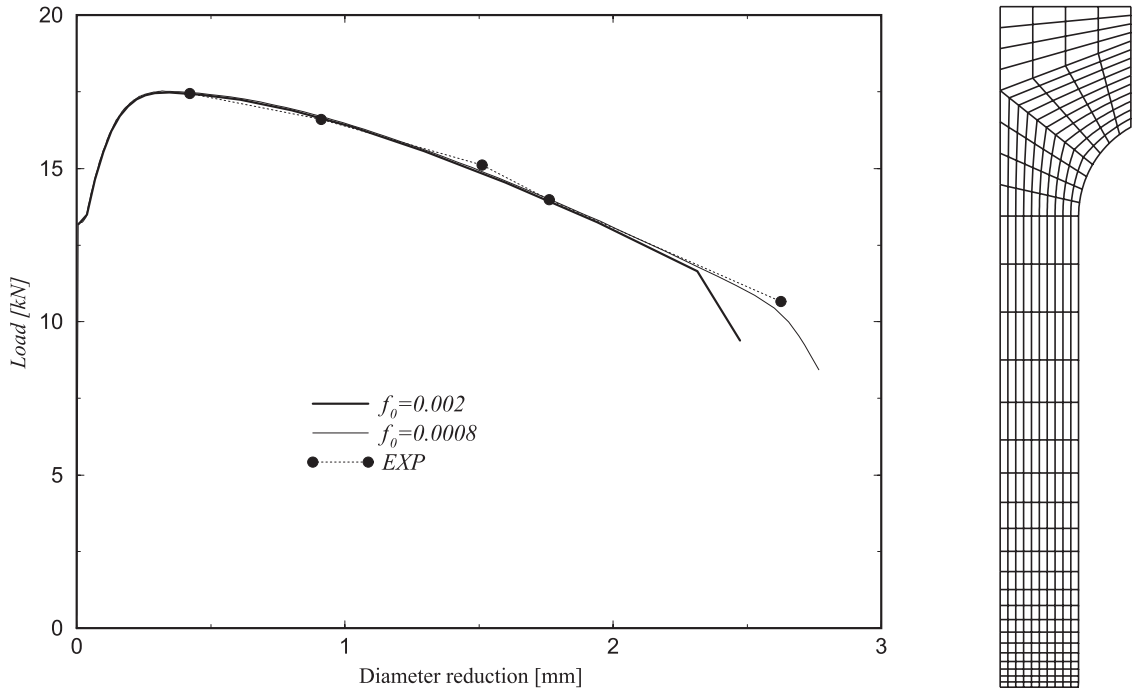

Fig. 4. Determination of the void nucleation parameter by using a single specimen geometry. The cluster void nucleation model was used. The finite element mesh is shown on the right side.

where G is the specimen geometry. When the ductility is known, the value of f_0 can be readily and uniquely determined. Fig. 4 shows an example from the second phase European round robin [18]. Only smooth tensile specimen results were available. The initial diameter was 6 mm. The experimental results are shown as filled circles. In the beginning, a trial value for f_0, of 0.002 as suggested in Ref. [18] was used. The complete Gurson model with this value predicts sudden load drop of the specimen (fracture point) much earlier compared with the experimental one. Another value $f_0 = 0.0008$ was used. Fig. 4 shows that the predicted load drop point with $f_0 = 0.0008$ is very close to the experimental one. So, $f_0 = 0.0008$ can be taken as the void nucleation parameter for the material.

In general, for the single specimen approach, the initial void volume fraction can be written as

$$f_0 = f_0(\varepsilon_f, G, n). \tag{9}$$

However, there is a problem for the single specimen approach. For the same experimental result, another nucleation model, for example, the continuous nucleation model, can be applied. By the same method, we can obtain A_0 as

$$A_0 = A_0(\varepsilon_f, G, n), \tag{10}$$

for the round robin material, we found that $A_0 = 0.0016$ gives a good fit to the experimental result, Fig. 5, and also yields almost identical result as $f_0 = 0.0008$ in Fig. 4. This is another type of non-uniqueness problem.

Actually, the predicted load–displacement curves by the two nucleation models are different, even though the predicted fracture strains are the same. Because of the nucleation parameters f_0 and A_0 are very

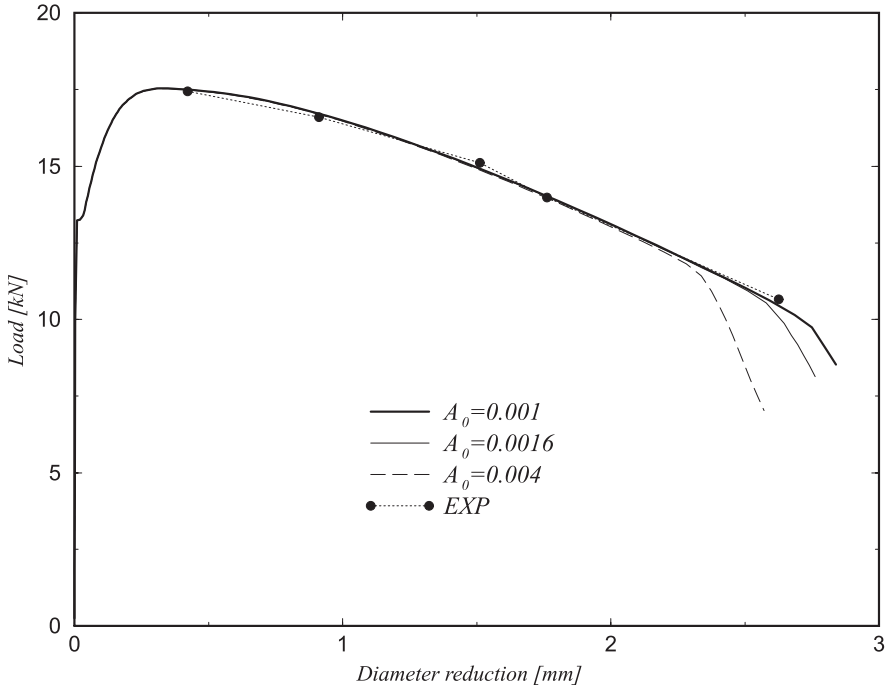

Fig. 5. Determination of the void nucleation parameter by using a single specimen geometry. The continuous nucleation model was used.

small for most engineering materials, the softening effect caused by the voids is not significant, and cannot be distinguished from experimental scatter.

3.2. Multispecimen approach

This above mentioned non-uniqueness problem can be solved by using multitension specimen – both smooth and notched specimens. The main argument is that multispecimens cover a wide range of stress triaxiality. If two nucleation models yield same results at smooth specimen (low triaxiality), they will certainly give different results at notched specimens (high triaxiality), vice versa. Fig. 6 shows the results

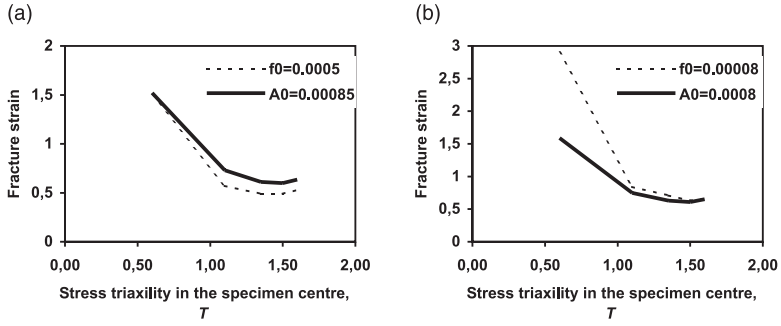

Fig. 6. The complete Gurson model: different nucleation models predict nearly the same ductility at one stress triaxiality but predict different ductilities at other stress triaxialities. The results are taken from analyses of a unit cell with constant stress triaxiality.

predicted by the complete Gurson model at different (constant) stress triaxiality. It can be seen that, different nucleation model yields different curvature in the fracture strain versus stress triaxiality diagram. In general, the cluster nucleation model results in steeper curvature than the continuous nucleation model.

When a ductility diagram (ductility versus a representative stress triaxiality from the specimen center) is known for a material, the cluster or the continuous model can be applied first. Different value of f_0 or A_0 will shift the predicted ductility versus stress triaxiality curve up and down. The one which fits best with the experimental results is the nucleation parameter for the material. When one nucleation model cannot give satisfactory fit for the given material, another nucleation model can then be tried. The method has been applied to a X65 pipe steel [19,20]. The diameter of the tensile specimen is 6 mm. Smooth specimen and specimens with notch radius $R = 2.0$, 1.2 0.8, and 0.4 mm were used. At first, the cluster nucleation model has been tried. It was found that this model does not give a good description for the steel. The continuous nucleation model was then tested. Fig. 7(a) shows the ductility diagram. In Fig. 7(a), the stress triaxiality was taken from the specimen center at fracture strain. The accurate value of stress triaxiality is not

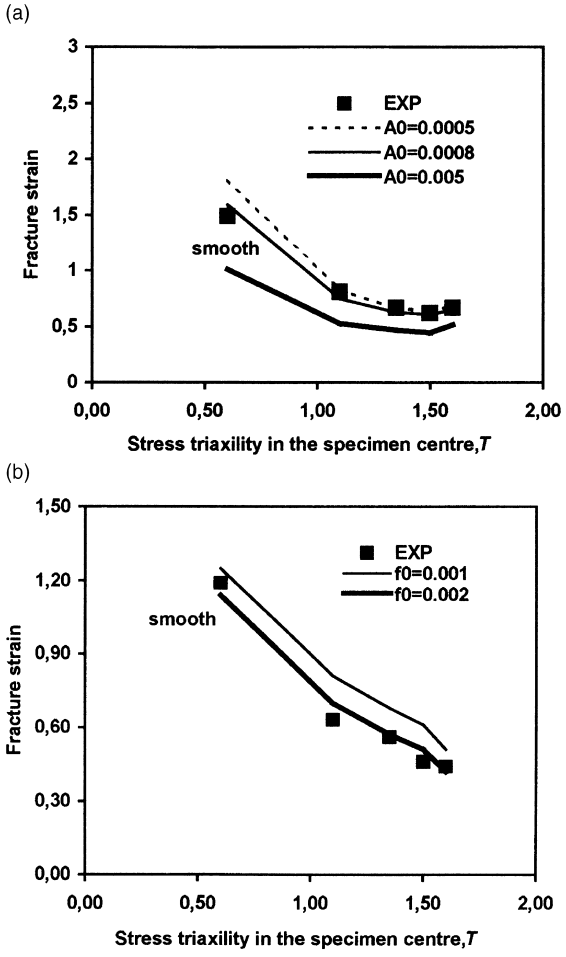

Fig. 7. Ductility diagram for determining the nucleation parameter: (a) for a X65 pipe steel, $A_0 = 0.0008$ gives a good fit to the experimental result, (b) for an Al–4.3%Si alloy, cluster nucleation model with $f_0 = 0.002$ fits the experimental result. One smooth and four notched tension specimens were used in both cases.

important. Three values of A_0, 0.0005, 0.0008 and 0.005 were analyzed. It can be seen that $A_0 = 0.0008$ gives the best fit to the experimental results. This example indicates that according to the complete Gurson model voids are nucleated from large and small inclusions/particles through the whole plastic deformation process in this pipe steel. The method has also been applied to an idealized Al–3.4%Si alloy [19,21]. Specimens with a 4 mm diameter were used. The same notch radius as that of the steel has been used for the notched specimens. The results are shown in Fig. 7(b). It was found that the cluster nucleation model with $f_0 = 0.002$ fits very well with the experimental results. It was very interesting to find from metallurgical examination that this alloy contains non-negligible initial defects and the volume fraction of the defects is close to 0.002. This indicates that the initial defects in this alloy are controlling the ductility.

In practice, one smooth and three different notched specimens can be used. The notch radius should be small enough so that high stress triaxiality will be tested. On the other hand, the notch radius should not be too small, so small that it acts like a crack. The purpose to use tension specimens is that the strain gradient in these specimens is relatively low and the effect of mesh size which is a direct representation of the material characteristic length parameter is not significant. For steels, one or two parallel tests for each specimen geometry may be enough, while for aluminum alloys, three parallels are usually needed [21].

4. Ductile crack resistance behavior

As noted initially, in tension specimens, the strain gradient is relatively low and the fitted void nucleation parameter is not very sensitive to the mesh size. For cracked specimens where the strain gradient is very high at the crack tip, the predicted crack resistance depends strongly on the mesh size. However, the shape of the resistance curves is determined by the void nucleation parameter. When the nucleation parameter is determined from the tension tests, in principal, the shape of the resistance curve is known. Fig. 8 shows the mesh size effect on the crack resistance curve for a three-point-bending specimen, with $a/w = 0.5$, and $w = 20$ mm. A very fine global mesh with four-node ABAQUS plane strain elements were used in the analyses. The material analyzed is a power strain hardening material with hardening exponent $n = 0.1$, void nucleation parameter $A_0 = 0.0008$, $\alpha = 0.1$, $q_1 = 1.5$, and $q_2 = 1.0$ (see also Fig. 6 and Ref. [20]). Five different mesh size, ranging from 0.05–0.15 mm were considered. A special zooming technique was applied to generate the mesh from a reference finite element model, the model with mesh size $l_c = 0.1$ mm, so that all the five models have exactly the same mesh pattern. No blunting was accounted for in Fig. 8. The crack growth was defined by $f = f_F$. The general observation from Fig. 8(a) is that crack resistance increases

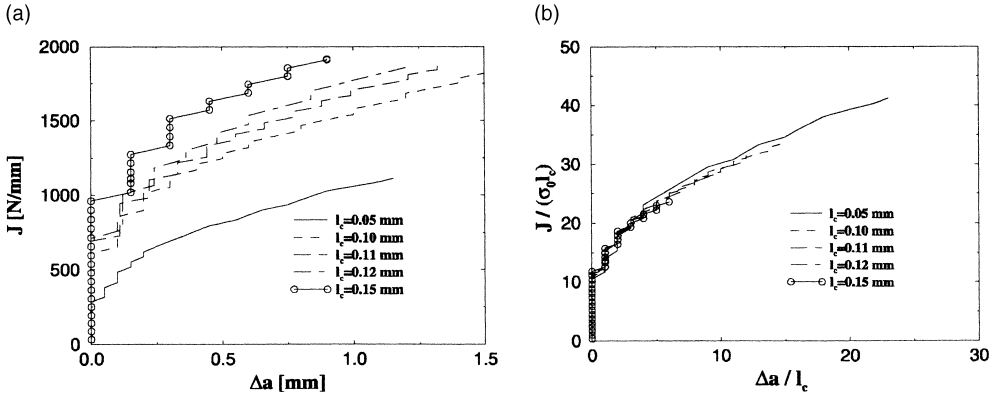

Fig. 8. The mesh size effect on the crack resistance behavior of a three-point-bending specimen.

when the mesh size increases. Fig. 8(b) shows, however, that the effect of crack tip mesh size can be normalized by the mesh size and mesh size scales the crack resistance curve. The same behavior has been observed for cluster nucleation law. The actual mesh size parameter can be fitted by comparing predicted resistance curves with different mesh sizes with the experimental crack resistance curve. If a zooming technique is used, new model with a different crack tip mesh can be easily generated from a reference mesh.

When the nucleation parameter and the mesh size for a material has been determined, they can now be transferred from one geometry to another, i.e. according to the complete Gurson model, they are the transferable parameters for ductile fracture. The crack resistance curve can be then written as

$$J = J(f_0, l_c, G, \Delta a), \tag{11}$$

where G represents the geometry factor. It is interesting to investigate if the geometry factor can be represented by a known parameter.

Modified boundary layer (MBL) models with different T stress applied at the remote boundary have been analyzed. Fig. 9(a) and (b) shows that the global mesh and local mesh for the MBL models, respectively. There are 40 regular elements in front of the crack tip. Fig. 9(c) shows the predicted crack resistance curves at different T stress levels for a material with $f_0 = 0.002$, hardening exponent $n = 0.1$, $\alpha = 0.1$, $q_1 = 1.5$, and $q_2 = 1.0$, and mesh size, $l_c = 0.1$ mm. It can be seen that the crack resistance increases when the T stress decreases (loss of constraint). We can also observe that the crack resistance curves look very similar to each other. A normalization procedure has been applied to the curves shown in Fig. 9(c) – all the curves are normalized by its value at 1 mm crack growth, and the results are shown in Fig. 9(d). Surprisingly, all the curves collapsed into one (except in the beginning of the crack growth). Fig. 10 shows the normalized quantities as a function of the T stress. It is interesting to observe that the resistance

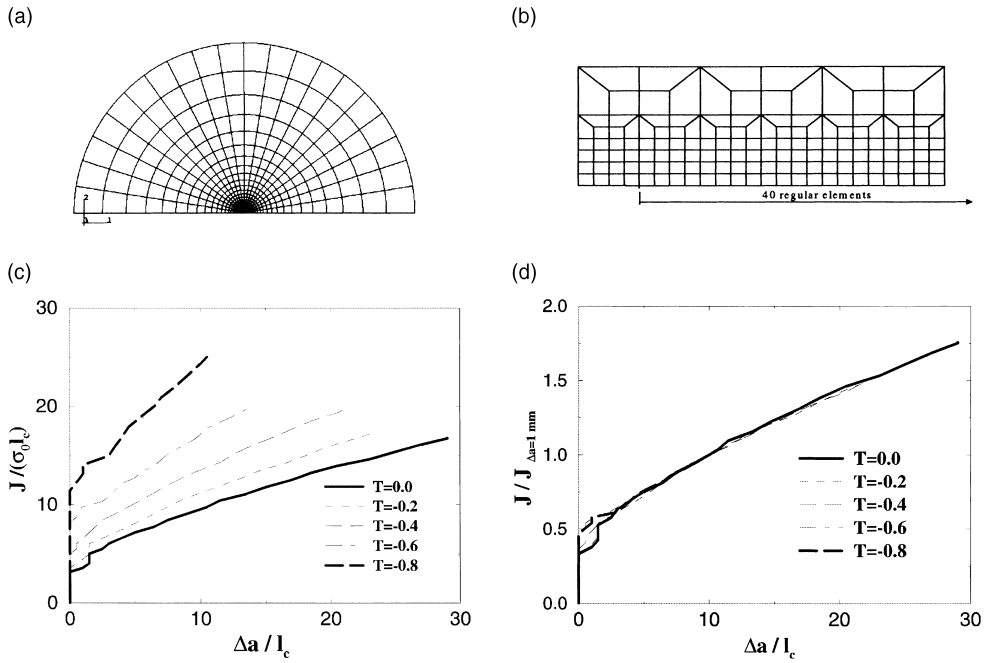

Fig. 9. (a) MBL model global mesh, (b) local mesh, (c) crack resistance curves at different T stresses, and (d) normalized resistance curves.

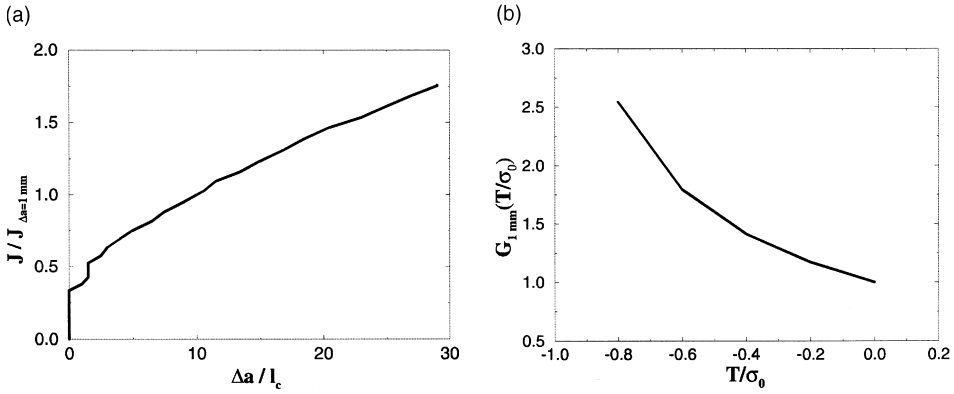

Fig. 10. (a) The reference resistance curve and (b) the geometry function for the MBL models shown in Fig. 9.

curves can be normalized by a function of the T stress, i.e., the crack resistance can be separated into two parts,

$$J = J_0(f_0, l_c, \Delta a)G_1(T), \tag{12}$$

where J_0 is the reference crack resistance for $T = 0$ and G_1 is the geometry function at 1 mm crack growth. For the MBL material, the J_0 and G_1 are shown in Fig. 10.

It should be noted that the results in Fig. 9(c) may seem to be in contradiction with experimental observations. It has been a common sense that crack initiation toughness of conventional steels is to a large extent insensitive to crack size (limited range of variation) or specimen geometry. In fact, Fig. 9(c) cannot be directly compared with experimental results. In the former, a constant T stress was applied, while in the later the T stress is a function of load. Similar results can be seen in the work of Burstow and Howard [22]. Even not as significant as we have shown, there is certainly an effect of T stress on the fracture initiation toughness.

5. Summary and discussion

The main purpose of the paper is to identify and possibly separate the transferable parameters for ductile fracture and the parameter which describe geometry effect. Cylindrical tension specimens including both smooth and notched specimens where the strain gradient is relatively low, and cracked specimens where strain gradient is very high at the crack tip were treated separately. According to the complete Gurson model where the so-called critical void volume fraction has been eliminated from material constants, ductile failure is one-to-one linked to the void nucleation parameter. The transferable parameter for tension specimens is thus the void nucleation parameter.

For cracked specimens, an extra parameter – the mesh size which describes the strain gradient effect should be determined. In this paper, we assume that the nucleation parameter can be directly transferred from tension specimens to the cracked specimens. That implies, the shape of the crack resistance curves is determined by the nucleation parameter from tension specimens. Because the mesh size scales the crack resistance curve as shown in Fig. 8, the "exact" mesh size can be determined by comparing the predicted crack resistance curves with the experimental one.

In practice, the crack resistance shape predicted by using the nucleation parameter from tension tests maybe different to the experimental one. There are several factors which may contribute to this discrepancy. For example, how to compare the 2D plane strain numerical resistance curve with 3D experimental curve.

We are currently working on the X65 steel where the base metal, weld metal and the heat affected zone materials have been tested. The results will be reported elsewhere.

For well defined crack problems – the MBL models, the ductile crack resistance behavior has been shown to be a function of the nucleation parameter, mesh size and the T stress. For constant T stress, a crack resistance curve can be calculated from the reference curve of the material multiplied by a T stress function.

Two simple nucleation models have been proposed. For either the cluster or continuous nucleation model, its parameter can be uniquely determined. The authors have found that the simple nucleation models work for many engineering materials. It has been shown that the continuous nucleation model even works for the X65 pipe steel, which is rather clean. In this material, not only the large inclusions but also the carbides may nucleate voids. The continuous nucleation model represents the average behavior of the nucleation mechanisms.

For some materials, it is possible that neither the cluster or the continuous nucleation model works. In such a case, a combination of the two models or the more sophisticated nucleation model by Chu and Needleman [14] may be applied. As pointed out in Ref. [6], if the nucleation model contains more than one parameter, some parameter(s) should be determined beforehand. This is difficult and may turn out to be an arbitrary selection. This is what exactly needs to be avoided in this paper by introducing simple nucleation models.

In spite of the fact that the complete Gurson model based approach looks attractive, we should be aware that there are several limitations of this approach. The complete Gurson model has been verified for cases with a small initial void volume fraction ($f_0 \leqslant 0.01$). A recent attempt on non-nodular cast iron [23] wherein the initial void volume fraction is close to 11%, shows that the complete Gurson model in the present form does not work on materials where the initial void volume fraction is high. It should also be noted that spherical voids have been assumed in the complete Gurson model. A recent work by Benzerga et al. [24] has shown that void shape may become important when stress triaxiality is low. The curvature in a ductility versus stress triaxiality diagram for tension specimens will somewhat become steeper when the void shape effect is considered in the complete Gurson model.

In this paper, fixed values of Tvergaard parameters q_1 and q_2 are applied. If Eq. (7) is used, the suggested values are $q_1 = 1.25$ and $q_2 = 1.0$. In general, q_1 and q_2 are also dependent on the hardening exponent. q_1 and q_2 as a function of n has tabulated in a recent study by Faleskog [25]. How different q_1 and q_2 values influence Eq. (7) will be studied and reported elsewhere.

It is obvious that studies are necessary to further verify the proposed approach. How to identify the geometry parameter – whether the T stress is still controlling ductile fracture in general crack specimens wherein the T stress is not constant is certainly one of the interesting topics worth pursuing.

Acknowledgements

The financial support from the Norwegian Research Council through the Strategic Institute Program at SINTEF is greatly appreciated. The authors are also grateful for the comments made by one of the reviewers on the cluster nucleation model.

References

[1] Gurson AL. Plastic flow and fracture behaviour of ductile materials incorporating void nucleation, growth and coalescence, PhD Diss, Brown University, 1975.

[2] Tvergaard V. Influence of voids on shear band instabilities under plane strain conditions. Int J Fract 1981;17:389–407.

[3] Tvergaard V. On localization in ductile materials containing spherical voids. Int J Fract 1982;18:237–52.
[4] Tvergaard V, Needleman A. Analysis of the cup-cone fracture in a round tensile bar. Acta Metall 1984;32:57–169.
[5] Sun D-Z, Kienzler R, Voss B, Schmitt W. Application of micro-mechanical models to the prediction of ductile fracture, Fracture Mechanics, 22nd Symposium, vol. II, ASTM STP 1131, In: Atluri SN, Newman JC Jr., Raju IS, Esptein JS, editors. American Society for Testing and Materials, Philadelphia, 1992. p. 368–78.
[6] Zhang ZL, Hauge M. On the Gurson parameters, Fatigue and Fracture Mechanics, vol. 29, ASTM STP 1321, In: Panontin TL, Sheppard SD, editors. American Society for Testing and Materials, 1998.
[7] Koplik J, Needleman A. Void growth and coalescence in porous plastic solids. Int J Solids Struct 1988;24:835–53.
[8] Zhang ZL. A complete Gurson model. Nonlinear fracture and damage mechanics, In: Aliabadi MH, editor. Computational Mechanics Publications, 1998.
[9] Thomason PF. Ductile fracture of metals. Pergamon Press, Oxford, 1990.
[10] Thomason PF. A three-dimensional model for ductile fracture by the growth and coalescence of micro-voids. Acta Metall 1985;33:1087–95.
[11] Thomason PF. A view on ductile-fracture modelling. Fatig Fract Engng Mat Struct 1998;21:1105–22.
[12] Gurland J. Observation on the fracture of cementie particles in a spheroidized 1.05 C steel deformed at room temperature. Acta Metall 1972;20:735–41.
[13] Caceres CH, Griffiths JR. Damage by the cracking of silicon particles in an Al–7Si–0.4Mg casting alloy. Acta Metall 1996;44:25–33.
[14] Chu CC, Needleman A. Void nucleation effects in biaxially stretched sheets. J Engng Mater Technol 1980;102:249–56.
[15] Zhang ZL. A micro-mechanical model based local approach methodology for the analysis of ductile fracture of welded T joints. PhD Thesis, Lappeenranta University of Technology, Finland, 1994.
[16] Pardoen T, Hutchinson JW. An extended model for void growth and coalescence, submitted for publication (2000).
[17] Ruggieri JW, Dodds RH. A transferability model fro brittle fracture including constraint and ductile tearing effects: a probablistic approach. Int J fract 1996;79:309–40.
[18] Bernauer G, Brocks W. ESIS TC8 Numerical Round Robin on micromechanical models, Phase II, 1998.
[19] Zhang ZL, Ødegård J, Thaulow C. Characterization of material ductility by microvoid nucleation parameters. In: Cvarstensen JV, et al., editors. Proceeding of the 19th Risø International Symposium on material science: Modelling of structure and mechnaics of materials from microscale to product, Risø, Denmark, 1998.
[20] Taule Å. Quantification of ductile crack growth in pipelines by means of damage mechanics calculations. MSc Thesis, NTNU, 1997 [in Norwegian].
[21] Ødegård J. Quantification of damage parameter and void volume fraction SINTEF report STF24 A97323, 1997 [in Norwegian].
[22] Burstow MC, Howard IC. Predicting of effects of crack tip constraint on material resistance curves using ductile damage theory. Fatig Fract Engng Mater Struct 1996;19:461–74.
[23] Steglich D. 1998, private communications.
[24] Benzerga A, Besson J, Pineau A. Coalescence-controlled anisotropic ductile fracture. J Engng Mater Technol, submitted for publication (2000).
[25] Faleskog J, Gao X, Shih CF. Cell model for nonlinear fracture mechanics-I micromechanics calibration. Int J Fract 1998;89:355–73.